Journal of Alloys and Compounds 509S (2011) S736–S739

Contents lists available at ScienceDirect

Journal of Alloys and Compounds

journal homepage: www.elsevier.com/locate/jallcom

Fast and slow dehydrogenation of ball milled lithium alanate ($LiAlH_4$) catalyzed with manganese chloride ($MnCl_2$) as compared to nanometric nickel catalyst

R.A. Varin*, L. Zbroniec

Department of Mechanical and Mechatronics Engineering, University of Waterloo, Waterloo, Canada N2L 3G1

ARTICLE INFO

Article history:
Received 16 July 2010
Received in revised form 4 September 2010
Accepted 8 September 2010
Available online 22 September 2010

Keywords:
Solid state hydrogen storage
Hydrogen storage materials
Lithium alanate ($LiAlH_4$)
Manganese chloride ($MnCl_2$)
Ball milling
X-ray diffraction (XRD)
Differential scanning calorimetry (DSC)

ABSTRACT

The results of the studies on the dehydrogenation behavior of the ball milled $LiAlH_4$ catalyzed with 5 wt.% of manganese chloride ($MnCl_2$) are reported. During ball milling for 15 min the $LiAlH_4$ + 5 wt.% $MnCl_2$ nanocomposite releases a miniscule amount of ~0.25 wt.% H_2. However, no products of the possible reaction between $LiAlH_4$ and $MnCl_2$ (e.g. LiCl) are observed by X-ray diffraction (XRD). In a DSC test most of $LiAlH_4$ decomposes exothermically to Li_3AlH_6 in a solid state while a small fraction of retained $LiAlH_4$ melts and decomposes in a liquid state. During dehydrogenation at 100 °C under 0.1 MPa H_2 the ball milled $LiAlH_4$ + 5 wt.% $MnCl_2$ nanocomposite is able to desorb ~4.6 wt.% H_2 within ~30,000 s in a solid state but only in Stage I (reaction: $LiAlH_4$ (solid) → $1/3Li_3AlH_6 + 2/3Al + H_2$). The apparent activation energy of dehydrogenation for this solid state reaction is equal to ~80 kJ/mol as compared to ~70 kJ/mol obtained for $LiAlH_4$+5 wt.% n-Ni [7]. However, during decomposition at 100 °C a chemical reaction occurs between $LiAlH_4$ and $MnCl_2$ producing LiCl and most likely an amorphous Mn metal catalyzing the reaction in Stage I. The ball milled $LiAlH_4$+5 wt.% $MnCl_2$ nanocomposite is capable of desorbing substantial quantities of H_2 during long term storage at room temperature (RT; ~21 °C), 40 and 80 °C.

1. Introduction

In the future Hydrogen Economy a viable solid state hydrogen storage system is needed for efficient supply of pure hydrogen to fuel cells in automotive and a variety of non-automotive applications like, for example, electronic consumer goods. For a Proton Exchange Membrane (PEM) fuel cell stack a viable hydrogen system requires operating temperature range roughly from room temperature (RT) to 100 °C and a practical hydrogen capacity exceeding at least 6 wt.% particularly for automotive applications [1].

One of the most interesting hydrides for solid state hydrogen storage is a complex metal hydride $LiAlH_4$ (lithium alanate) since it can liberate a theoretical quantity of 7.9 wt.% H_2 below 250 °C [1]. $LiAlH_4$ releases only high purity H_2 in contrast to complex metal borohydrides that can also release diboranes [1] which are destructive to a fuel cell's membrane. Some catalytic metal chlorides such as $TiCl_3$ [2,3], $ZrCl_4$ [4], VCl_3 [4,5], $NiCl_2$ [4,6] and $ZnCl_2$ [4] were added to $LiAlH_4$ which enhanced quite dramatically the rate of desorption and in effect lowered the effective desorption temperature of $LiAlH_4$.

In the present work we report the results of the studies on the dehydrogenation behavior of the ball milled $LiAlH_4$ catalyzed with 5 wt.% of manganese chloride ($MnCl_2$). The emphasis is on the dehydrogenation behavior at a temperature range from RT to 100 °C which roughly falls within the operating temperature range of a PEM fuel cell. The results are qualitatively compared to the catalytic effects of nanometric nickel (n-Ni) which are already reported in [7,8]. The latter results are treated as a benchmark for comparison. It is to be pointed out that the catalytic effects of $MnCl_2$ on the dehydrogenation behavior of $LiAlH_4$ have never been investigated.

2. Experimental

$LiAlH_4$ of 97% purity (Alfa Aesar) which was thoroughly characterized in [9] was mixed with 5 wt.% of the $MnCl_2$ catalytic precursor (99.99% pure, ultra dry manganese(II) chloride ($MnCl_2$) from Alfa Aesar) and subsequently processed by controlled ball milling for 15 min in the magneto-mill Uni-Ball-Mill 5 under high energy impact mode IMP68 with two magnets [1,7–11]. The ball-to-powder weight ratio (R) used in this work was 132:1 (R132) as opposed to both 40:1 (R40) and R132 used for the system $LiAlH_4$ + 5 wt.% n-Ni in [7]. In our research on the dehydrogenation of various hydrides we have found no measurable difference in the investigated microstructural and hydrogen storage properties between hydride powders processed with these two R's and eventually we set up at R132 as it saves the quantity of powder used. The rotational speed of milling vial was ~200 rpm. The processed nanocomposite powders were investigated by differential scanning calorimetry (DSC), X-ray diffraction (XRD) and volumetric hydrogen desorption in a Sieverts-type apparatus. Due to the space limitation an interested reader can find the details of all the experimental techniques in our most recent publications [1,7–11]. For the long-term storage experiments at room temperature (RT; ~21 °C), 40 and 80 °C the

* Corresponding author. Tel.: +1 519 888 4567; fax: +1 519 885 5862.
E-mail addresses: ravarin@uwaterloo.ca, ravarin@mecheng1.uwaterloo.ca (R.A. Varin).

0925-8388/$ – see front matter © 2010 Elsevier B.V. All rights reserved.
doi:10.1016/j.jallcom.2010.09.068

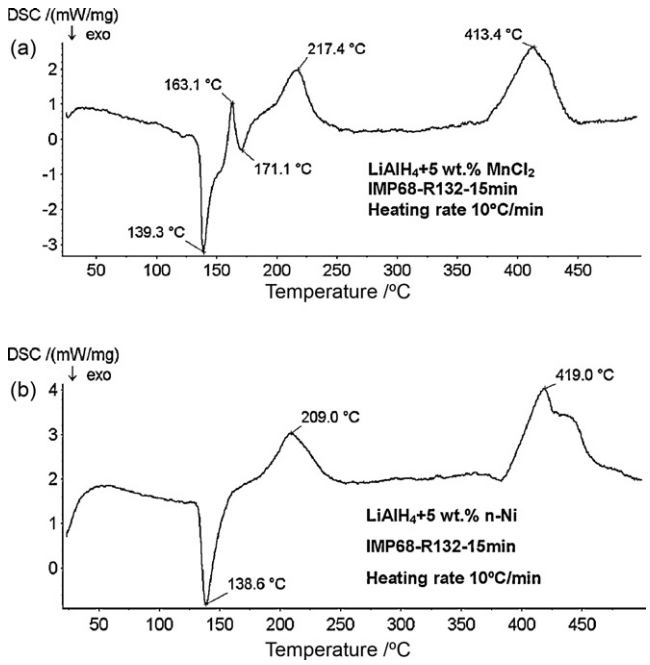

Fig. 1. Comparison of DSC curves for catalyzed $LiAlH_4$ ball milled under IMP68 for 15 min with R132. (a) $LiAlH_4$ + 5 wt.%$MnCl_2$ (this work). (b) $LiAlH_4$ + 5 wt.% n-Ni [7].

ball milled $LiAlH_4$ + 5 wt.% $MnCl_2$ nanocomposite was stored under 0.1 MPa pressure of high purity argon (99.999% purity) in a tightly sealed glass vial at a prescribed temperature (at RT in a glove box and at 40 and 80 °C in an oven). A small quantity of powder was extracted from a vial after a predetermined number of storage days in a glove box filled up with high purity argon. A characteristic "pop up" sound was always heard after opening the vial which indicated a hydrogen pressure build up inside the sealed vial. Subsequently, the extracted powder sample was loaded in a glove box into a tightly sealed reactor chamber which was mounted in a furnace of our Sieverts type apparatus. After purging a few times with vacuum/H_2 the final pressure of 0.1 MPa H_2 was set up in the reactor and the powder was fully dehydrogenated at 170 °C. A hydrogen desorption curve was registered until full saturation was reached (usually up to 10–20 ks).

3. Results and discussion

SEM observations show that the average particle size after ball milling is on the order of ~3 μm as compared to the initial average particle size of as received $LiAlH_4$ which is equal to ~10 μm [9]. Grain/crystallite size estimate of $LiAlH_4$ from the peak breadths of Bragg peaks in XRD patterns, following the methodology described in [1,7–11], shows that the average grain size of ball milled $LiAlH_4$ is close to ~80 nm with an excellent coefficient of fit R^2 of about 0.96–0.98. Therefore, we refer to these ball milled catalyzed powders as nanocomposites. Pressure drop measurements in a milling vial in due course of milling were conducted from which a loss of about 0.25 wt.% H_2 after 15 min of ball milling was estimated according to the procedures described in [1]. The XRD pattern of a ball milled nanocomposite $LiAlH_4$ + 5 wt.% $MnCl_2$ (not shown here) exhibits only majority peaks of $LiAlH_4$ (JCPDS#73-0461) as well as peaks of the Al minority phase (JCPDS#85-1327) which is most likely an impurity [9]. A very weak peak at the 2θ position which may correspond to the 100% (0 2 0) peak of Li_3AlH_6 (JCPDS#27-0282) is also observed but this position is also superimposed with the 19% (-1 1 1) peak of $LiAlH_4$ so it is hard to conclude unambiguously whether or not some minutiae quantity of Li_3AlH_6 is indeed present in the microstructure after milling. However, no products of the reaction between $LiAlH_4$ and $MnCl_2$ are observed by XRD. In addition, no 100% (0 0 3) peak of $MnCl_2$ (JCPDS#22-0720) could be recognized in the XRD pattern after milling which suggests that $MnCl_2$ may have become amorphous as a result of milling.

Fig. 1a shows a DSC curve for ball milled $LiAlH_4$ + 5 wt.% $MnCl_2$. The low temperature of the first exothermic peak at 139.3 °C strongly indicates that, most likely, this peak may represent a superposition of two events as discussed in [7,9]. The first one is the reaction of the surface aluminum-hydroxyl groups owing to the presence of impurities as first reported by Block and Gray [12]. As also recently suggested in [7,9] this hydroxyl reaction may possibly trigger the second event which is the decomposition of $LiAlH_4$ in a solid state according to the well-known reaction which theoretically releases about 5.3 wt.% H_2 [1]:

$$LiAlH_4(solid) \rightarrow 1/3Li_3AlH_6(solid) + 2/3Al(solid) + H_2 \quad (1)$$

However, this reaction seems not to proceed to a full completion because a small fraction of retained $LiAlH_4$ melts (notice a small endo peak at 163.1 °C) and immediately afterwards decomposes according to reaction (1) in a liquid state at the exothermic peak around 171.1 °C (Fig. 1a). However, the most recent results obtained in our laboratory show that the increase of $MnCl_2$ content to about 29 wt.% in the ball milled nanocomposite (molar ratio $8LiAlH_4 + MnCl_2$) completely eliminates melting of $LiAlH_4$.

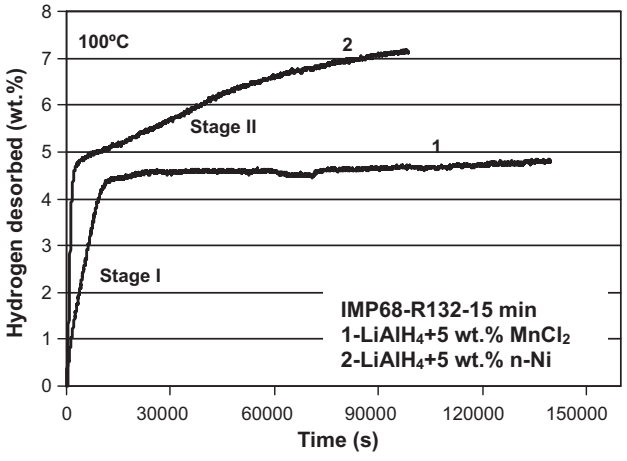

Fig. 2. Comparison of volumetric desorption curves at 100 °C under 0.1 MPa H_2 for catalyzed $LiAlH_4$ ball milled under IMP68 for 15 min with R132. 1-$LiAlH_4$ + 5 wt.%$MnCl_2$ (this work) (desorbed up to 140 ks) and 2-$LiAlH_4$ + 5 wt.% n-Ni (desorbed up to 98 ks) [7].

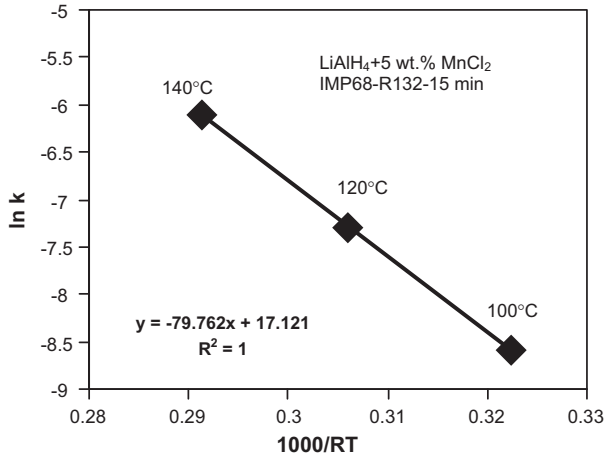

Fig. 3. The Arrhenius plot of rate constant k with temperature for estimation of the apparent activation energy of hydrogen desorption for the ball milled $LiAlH_4$ + 5 wt.% $MnCl_2$ system for Stage I.

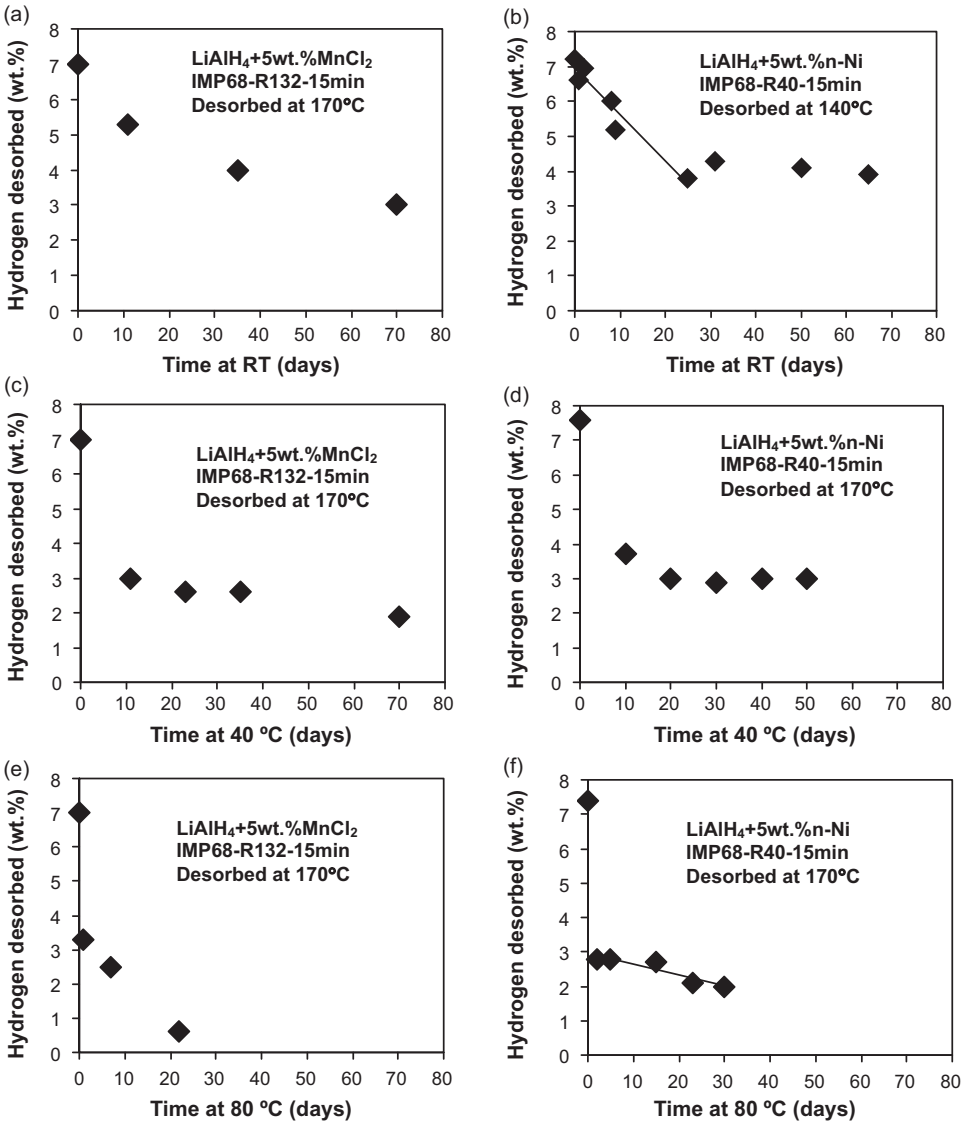

Fig. 4. Comparison of the amounts of hydrogen desorbed during long term storage at room temperature (RT), 40 and 80 °C for (a, c and e) ball milled $LiAlH_4$ + 5 wt.% $MnCl_2$ (this work) and (b, d and f) $LiAlH_4$ + 5 wt.% n-Ni [7].

As can be seen in Fig. 1b, in contrast to $MnCl_2$, the addition of 5 wt.% n-Ni to $LiAlH_4$ combined with a high energy ball milling completely eliminates melting of $LiAlH_4$ in a DSC test. It must, however, be pointed out that just mixing of $LiAlH_4$ with the same amount of n-Ni does not eliminate melting at all as reported in [7]. The endothermic peaks at 217.4 and 209 °C observed in Fig. 1a and b for $LiAlH_4$ + 5 wt.% $MnCl_2$ and $LiAlH_4$ + 5 wt.% n-Ni, respectively, are due to a well-known second major reaction in a solid state according to the following path which theoretically releases about 2.6 wt.%H_2 [1]:

$$1/3Li_3AlH_6 \rightarrow LiH + 1/3Al + 0.5H_2 \quad (2)$$

High temperature peaks at 413.4 °C and 419 °C observed in Fig. 1a and b for $LiAlH_4$ + 5 wt.% $MnCl_2$ and $LiAlH_4$ + 5 wt.% n-Ni, respectively, are customarily assigned to the decomposition of LiH [1]. As very recently reported in [8] the formation of various intermetallic compounds in the ball milled $LiAlH_4$ + 5 wt.% n-Ni system is also observed around this peak temperature so the origin of this peak is rather ambiguous.

Ball milled $LiAlH_4$ + 5 wt.% n-Ni desorbs relatively fast at the 140–250 °C range under 0.1 MPa H_2 (atmospheric pressure) the quantity of about 7.4–7.8 wt.% H_2 within 10,000–600 s, respectively [7,8]. In contrast, ball milled $LiAlH_4$ + 5 wt.% $MnCl_2$ desorbs at the same temperature range with a slightly lower rate the quantity of 6.7–7.2 wt.%H_2 within 20,000–600 s, respectively.

Fig. 2 shows a comparison of isothermal volumetric hydrogen desorption curves obtained at 100 °C under 0.1 MPa H_2 for ball milled $LiAlH_4$ + 5 wt.% $MnCl_2$ up to 140 ks and $LiAlH_4$ + 5 wt.% n-Ni up to 98 ks desorption time. For the 5 wt.% $MnCl_2$ additive dehydrogenation occurs in a solid state but only through Stage I (reaction (1)) while for the 5 wt.% n-Ni additive, within a similar time span, dehydrogenation occurs in a solid state through both Stage I and II (reactions (1) and (2), respectively). After desorption of ball milled $LiAlH_4$ + 5 wt.% $MnCl_2$ at 100 °C for 140 ks its XRD pattern (not shown here) exhibits the diffraction peaks of LiCl (JCPDS#04-0664), Al and Li_3AlH_6. Apparently, during decomposition besides reaction (1) in Stage I producing Li_3AlH_6 and Al a second reaction producing LiCl (and again Al) must have occurred with the following general path:

$$nLiAlH_4 + MnCl_2 \rightarrow (n-2)LiAlH_4 + 2LiCl + 2Al + Mn + 4H_2 \quad (3)$$

For 5 wt.% $MnCl_2$, $n = 63$ so the exact reaction is as follows:

$$63LiAlH_4 + MnCl_2 \rightarrow 61LiAlH_4 + 2LiCl + 2Al + Mn + 4H_2 \quad (4)$$

Since no diffraction peaks of Mn (JCPDS# 33-0887/32-0637) are observed after desorption at 100 °C for 140 ks most likely Mn is in an amorphous state.

Apparently, dehydrogenation rate of $LiAlH_4$ + 5 wt.% $MnCl_2$ is slower than that for its counterpart with the 5 wt.% n-Ni additive. The apparent activation energy of dehydrogenation for Stage I for $LiAlH_4$ + 5 wt.% $MnCl_2$ has been estimated using the Johnson–Mehl–Avrami–Kolmogorov (JMAK) and Arrhenius equations according to the methodology described in detail in [1,7–11]. Fig. 3 shows the Arrhenius plot for three temperatures used for calculations which renders the value of ~80 kJ/mol with an excellent coefficient of fit R^2. This value can be compared to a value of ~70 kJ/mol for Stage I obtained for $LiAlH_4$ + 5 wt.% n-Ni in [7].

At this point it is appropriate to elucidate the effect of ball milling and resulting nanostructuring on $LiAlH_4$ without any catalytic additives. It is found that the apparent activation energy of dehydrogenation for unmilled (as received) LiAlH4 is equal to ~111 and ~100 kJ/mol for reactions (1) and (2), respectively [9]. For ball milled $LiAlH_4$ the apparent activation energy of dehydrogenation is slightly reduced to ~92.5 and ~92 kJ/mol for reactions (1) and (2), respectively [9]. In addition, Fig. 9 in [7] shows that at 100 °C under 0.1 MPa H_2 pressure about 5 wt.%H_2 is desorbed within 70,000 s and 270,000 s for ball milled and unmilled (as received) $LiAlH_4$, respectively. Apparently, ball milling of $LiAlH_4$ is definitely beneficial for improvement of its dehydrogenation kinetics but still the nanometric catalytic additives bring about an additional profound improvement in the dehydrogenation kinetics.

Fig. 4 shows the comparison of the amount of hydrogen desorbed during long term storage at room temperature (RT; ~21 °C), 40 and 80 °C for ball milled $LiAlH_4$ + 5 wt.% $MnCl_2$ (Fig. 4a, c and e) and $LiAlH_4$ + 5 wt.% n-Ni (Fig. 4b, d and f). It can be seen that the ball milled $LiAlH_4$ + 5 wt.% $MnCl_2$ nanocomposite is able to desorb substantial quantities of H_2 at these low temperatures. At RT and 80 °C the ball milled $LiAlH_4$ + 5 wt.% $MnCl_2$ nanocomposite within a comparable time span slowly desorbs even slightly greater amount of H_2 than its $LiAlH_4$ + 5 wt.% n-Ni counterpart despite that at elevated temperatures the apparent activation energy of 5 wt.% $MnCl_2$ doped $LiAlH_4$ is slightly greater (~80 vs. ~70 kJ/mol, respectively).

4. Conclusions

During high energy ball milling for 15 min the $LiAlH_4$ + 5 wt.% $MnCl_2$ nanocomposite releases about 0.25 wt.% H_2. However, no products of any possible reaction of $LiAlH_4$ with $MnCl_2$ (e.g. LiCl) are observed on the corresponding XRD pattern. In contrast, the $LiAlH_4$ + 5 wt.% n-Ni nanocomposite does not release H_2 during high energy milling up to 1 h [7]. In a DSC test the majority of $LiAlH_4$ in the $LiAlH_4$ + 5 wt.% $MnCl_2$ nanocomposite decomposes exothermically to Li_3AlH_6 in a solid state reaction although a small amount of it is still retained which subsequently melts and simultaneously decomposes in a liquid state. During a volumetric desorption test in a Sieverts-type apparatus at 100 °C under 0.1 MPa H_2 pressure, ball milled $LiAlH_4$ + 5 wt.% $MnCl_2$ desorbs about ~4.6 wt.% H_2 within ~30,000 s (~4.8 wt.%H_2 within 140,000 s) in a solid state but only in Stage I (reaction (1)) as opposed to the $LiAlH_4$ + 5 wt.% n-Ni nanocomposite which desorbs slightly over 7 wt.% H_2 in both Stage I and II (reactions (1) and (2)) [7]. An XRD pattern of $LiAlH_4$ + 5 wt.% $MnCl_2$ desorbed at 100 °C exhibits diffraction peaks of LiCl which give evidence that a reaction between $LiAlH_4$ and $MnCl_2$ occurred during dehydrogenation. The apparent activation energy of dehydrogenation of ball milled $LiAlH_4$ + 5 wt.% $MnCl_2$ for Stage I is equal to ~80 kJ/mol as compared to ~70 kJ/mol for $LiAlH_4$ + 5 wt.% n-Ni in [7]. The ball milled $LiAlH_4$ + 5 wt.% $MnCl_2$ nanocomposite is able to desorb substantial quantities of H_2 at RT, 40 and 80 °C. At RT and 80 °C the ball milled $LiAlH_4$ + 5 wt.% $MnCl_2$ nanocomposite, within a comparable time span, seems to desorb a measurably greater amount of H_2 than its $LiAlH_4$ + 5 wt.% n-Ni counterpart.

Acknowledgments

This research was supported by the NSERC Hydrogen Canada (H2CAN) Strategic Research Network and NSERC Discovery grants which are gratefully acknowledged. The authors are grateful to Prof. Linda Nazar from the Department of Chemistry, University of Waterloo, for the usage of XRD equipment.

References

[1] R.A. Varin, T. Czujko, Z.S. Wronski, Nanomaterials for Solid State Hydrogen Storage, Springer Science+Business Media, New York, NY, 2009.
[2] M. Resan, M.D. Hampton, J.K. Lomness, D.K. Slattery, Int. J. Hydrogen Energy 39 (2005) 1413–1416.
[3] A. Andreasen, J. Alloys Compd. 419 (2006) 40–44.
[4] Y. Kojima, Y. Kawai, M. Matsumoto, T. Haga, J. Alloys Compd. 462 (2008) 275–278.
[5] J.R. Ares Fernandez, F. Aguey-Zinsou, M. Elsaesser, X.Z. Ma, M. Dornheim, T. Klassen, R. Bormann, Int. J. Hydrogen Energy 32 (2007) 1033–1040.
[6] T. Sun, C.K. Huang, H. Wang, L.X. Sun, M. Zhu, Int. J. Hydrogen Energy 33 (2008) 6216–6221.
[7] R.A. Varin, L. Zbroniec, J. Alloys Compd. 506 (2010) 928–939.
[8] R.A. Varin, L. Zbroniec, T. Czujko, Z.S. Wronski, Int. J. Hydrogen Energy (in press).
[9] R.A. Varin, L. Zbroniec, J. Alloys Compd. 504 (2010) 89–101.
[10] R.A. Varin, L. Zbroniec, Int. J. Hydrogen Energy 35 (2010) 3588–3597.
[11] R.A. Varin, T. Czujko, Z.S. Wronski, Int. J. Hydrogen Energy 34 (2009) 8603–8610.
[12] J. Block, A.P. Gray, Inorg. Chem. 4 (1965) 304–305.